Current Optics and Photonics
Vol. 2, No. 6, December 2018, pp. 606-611

ISSN: 2508-7266(Print) / ISSN: 2508-7274(Online)
DOI: https://doi.org/10.3807/COPP.2018.2.6.606

Estimation of the Ratio of Nonlinear Optical Tensor Components by Measuring Second Harmonic Generation and Parametric Down Conversion Outputs in a Single Periodically Poled $LiNbO_3$ Crystal

CH. S. S. Pavan Kumar, Jiung Kim, Byoung Joo Kim, and Myoungsik Cha*

Department of Physics, Pusan National University, Busan 46241, Korea

(Received September 10, 2018 : revised October 24, 2018 : accepted November 13, 2018)

Measurement of the nonlinear optical coefficients is not an easy task since it requires complicated experimental setup and analysis. We suggest an easy way to estimate the relative nonlinear optical tensor components by direct measurement of the output powers of the second harmonic generation and spontaneous parametric down conversion experiments. The experiments were done in quasi-phase-matched type-0 as well as type-1 interactions at similar pump wavelengths in a 5% MgO-doped periodically poled $LiNbO_3$ crystal to obtain the ratio of the nonlinear optical tensor components d_{33}/d_{31} in each experiment. The obtained ratios were then compared with the previously ascertained values [J. Opt. Soc. Am. B, 14, 2268-2294 (1997)].

Keywords : Harmonic generation, Quasi-phase-matching, Nonlinear optical coefficients
OCIS codes : (190.2620) Harmonic generation and mixing; (190.4410) Nonlinear optics, parametric process

I. INTRODUCTION

Ever since the invention of the laser and the first demonstration of second-harmonic generation (SHG) by Franken *et al*. [1], there has been an upsurge in the generation of light at desired frequencies via nonlinear optical devices. These developments have allowed us to exploit frequency ranges which were impossible when operating with conventional lasers. A key point in implementation of any nonlinear optical devices such as frequency doublers and optical parametric oscillators is to have an accurate estimate of the nonlinear optical coefficients on which any nonlinear process is eminently reliant. Meticulous assessment of its absolute value is crucial in order to have an in-depth knowledge of the involved nonlinear processes.

A significant material exploited for frequency conversion is lithium niobate ($LiNbO_3$) due to its large nonlinear coefficient and wide transparency range [2]. The development and implementation of quasi phase matching (QPM) devices such as periodically poled lithium niobate (PPLN) further accelerated its usage in various application such as RGB generation [3], projection display applications [4], molecular spectroscopy, environmental monitoring and military applications [5]. Unfortunately, $LiNbO_3$ is susceptible to photorefractive damage (PRD) which leads to optical damage and hence is not suitable for high power applications [2]. A way to deal with this is to use magnesium doped $LiNbO_3$ [6]. It was seen that 5% MgO:PPLN does not show PRD at very high input intensities even in the visible wavelength ranges [7, 8]. Hitherto, the absolute values of nonlinear coefficient of 5% MgO:PPLN have been reported by Eckardt *et al*. [9] and Shoji *et al*. [10]. Eckardt *et al*. performed temperature tuned critically phase-matched SHG in a 6.3 mm-long MgO:PPLN pumped at 1064 nm and reported the value of d_{31} to be 4.7 pm/V.

Shoji *et al*. used the non-phase-matched SHG wedge fringe method, Maker fringe method, and parametric fluorescence (PF) to determine the tensor components of the nonlinear coefficients. The d_{33} value was established using the wedge fringe method at 1064 nm and was found to be 25 pm/V. The Maker fringe (relative measurement against d_{33} of congruent $LiNbO_3$) experiment was done at 1064 nm

*Corresponding author: mcha@pusan.ac.kr, ORCID 0000-0002-5997-3881
Color versions of one or more of the figures in this paper are available online.

and ascertained that the d_{31} value was 4.4 pm/V. The d_{33} and d_{31} values were also found to be 28.4 pm/V and 4.4 pm/V, respectively, at 852 nm (fundamental) using the wedge fringe method. The PF method was done at 488 nm and established the d_{31} coefficient to be 4.9 pm/V.

It can clearly be seen that the d_{31} values at 1064 nm obtained by the two investigators seem to differ [9, 10]. A possible cause for the larger value of the former could be explained by multiple reflection effects in their experiment. The reflection effect was taken into account by Shoji *et al*. Another inconsistency is the larger value of d_{31} obtained by PF when compared to the one obtained from the SHG measurement. This discrepancy was also seen in nonlinear coefficient measurements of other crystals such as congruent $LiNbO_3$ [11, 12], $LiIO_3$ [9, 12], and KTP [13, 14].

Estimation of the d_{33}/d_{31} ratio is a must to have an idea of an input power level that would be required to produce a detectable SHG output in the type-1 nonlinear interactions when one already knows that for the conventional type-0 interaction. This ratio also plays a pivotal role in making quantifiable scrutiny of a nonlinear frequency conversion process which is crucial in estimating ideal circumstances and avoiding consequences that damage the conversion process [9]. According to Shoji *et al*. [10], this ratio turns out to be 5.68 at 1064 nm, and 5.79 at 852 nm. Their experimental procedures employed non-phase-matched techniques which produced weak signals and hence required a sensitive detector. This escalates the experimental cost and is also complicated when compared to the phased-matched experiments. Another disadvantage clearly seen is the discrepancy caused by the multiple reflection effects when the sample surfaces are not antireflection-coated.

To avoid these shortcomings, we obtained the d_{33}/d_{31} ratio by comparing the QPM type-0 and type-1 SHG outputs from a 5% MgO:PPLN. The SHG signals were very strong and could be detected easily with a common power meter and made the experiment procedure a lot easier. Since it is a comparison experiment, we can neglect multiple reflection effects and thereby avoiding any discrepancies. This gave us a $(d_{33}/d_{31})_{SHG}$ value. We further verified this ratio by performing spontaneous parametric down-conversion (SPDC) experiments. The obtained ratios in both the experiments were also in agreement with the earlier reported values.

II. EXPERIMENTS

A schematic diagram of our experimental setup is shown in Fig. 1(a). The nonlinear crystal used in the experiment was a z-cut 10-mm-long 5% MgO:PPLN. The crystal was mounted in an oven whose temperature could be varied from 25 to 130°C with an accuracy of 0.1°C. The QPM period was selected as 27.58 μm, according to the Sellmeier equations given by Gayer *et al*. [15]. This QPM period is expected to satisfy the following parametric interactions: (1) Type-0 ($e + e \rightarrow e$) 5th order QPM SHG of 990.6 nm at 55°C and its reverse SPDC process pumped at 495.3 nm. (2) Type-1 ($o + o \rightarrow e$) 1st order QPM SHG of 970.8 nm at 60°C and its reverse SPDC process pumped at 485.4 nm.

The pump beam was generated from an optical parametric generator-optical parametric amplifier (OPG-OPA) system using two β-barium borate (BBO) crystals which were pumped by the third harmonic (355 nm) of a mode-locked Nd:YAG laser (Quantel YG901, pulse width: 35 ps, repetition rate: 10 Hz) [3]. The output wavelength of the OPG-OPA system was tuned to either ~490 nm (signal) or ~980 nm (idler) as per the requirement, having a typical linewidth of ~4 nm. Appropriate filters were used to either transmit or block the signal/idler of the OPG-OPA system. A Fresnel rhombus was used to rotate the plane of polarization of the OPG-OPA output beam when necessary. It was then focused and propagated in the crystal along the crystalline x-axis. The $1/e^2$ beam radius at the focus was determined to be 250 μm by a scanning knife-edge experiment.

First, we performed temperature-tuned SHG experiments for type-0 and type-1 configurations in order to confirm the QPM conditions predicted by the temperature-dependent

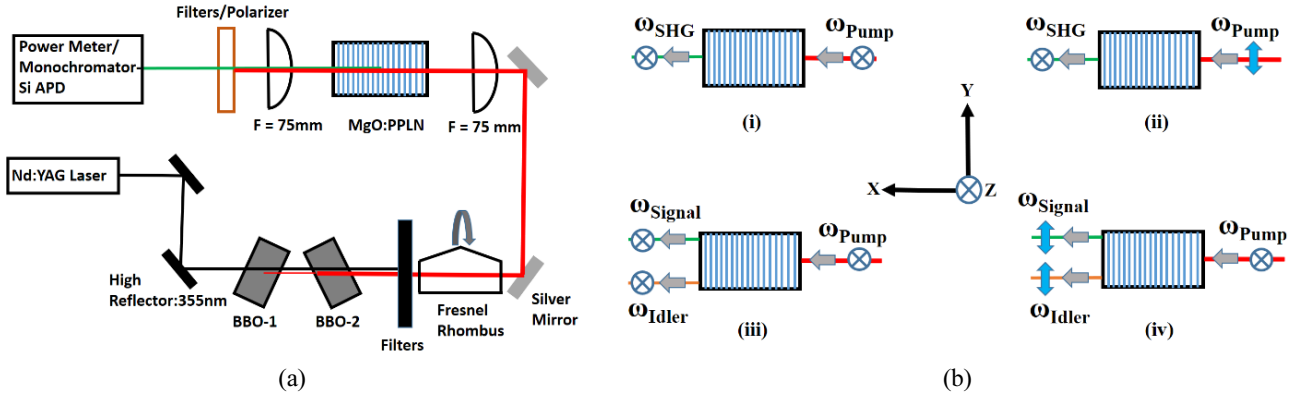

FIG. 1. Schematic of the experimental setup (a), and polarization configurations (b): (i) type-0 SHG, (ii) type-1 SHG, (iii) type-0 SPDC and (iv) type-1 SPDC. Gray arrows: propagation direction along x-axis, blue arrows and crossed circles: polarization directions.

Sellmeier equations [15]. In the case of the type-0 QPM SHG, the input (idler from the OPG-OPA) wavelength (ω_{Pump}) was tuned to 990.6 nm, and the polarization direction was aligned parallel to the z-axis of the crystal as shown in Fig. 1(b-i). The z-polarized SHG (ω_{SHG}) output, related to d_{33}, was directly measured with a pyroelectric detector. On the other hand, to obtain the type-1 QPM SHG from the same crystal, the input wavelength was tuned to 970.8 nm, and the polarization direction was aligned parallel to the y-axis of the crystal as in Fig. 1(b-ii). The z-polarized output was measured with the same pyroelectric detector. This z-polarized SHG output is related to d_{32} (= d_{31}), since for the 3 m point group, the effective nonlinearity for a uniaxial crystal is given by the expression [16],

$$d_{ooe} = d_{31}\sin(\theta) - d_{22}\cos(\theta)\sin(3\varphi), \quad (1)$$

where θ is the polar angle between z-axis and the wave vector which in our case is the crystalline x-axis, φ is the azimuthal angle. Since $\theta = 90°$, the contribution from d_{22} becomes zero, making $d_{ooe} = d_{31}$ for our type-1 SHG [16]. The ratio $(d_{33}/d_{31})_{SHG}$ was obtained by comparing the measured output power for the two configurations.

For inquisitiveness and verification, we performed the reverse of the SHG experiments i.e. SPDC. For the type-0 SPDC experiment, the OPG-OPA signal wavelength was tuned to 495.3 nm, while it was tuned to 485.4 nm for the type-1 SPDC. The pump (OPG-OPA signal) was polarized parallel to the z-axis in both cases. The output SPDC (ω_{Signal} and ω_{Idler}) signal was z-polarized in the type-0 SPDC and y-polarized in the type-1 SPDC as shown in Figs. 1(b-iii) and (b-iv), respectively.

Among the SPDC outputs from the MgO:PPLN crystal, the signal part was spectrally separated by a monochromator, and measured with a silicon avalanche photodiode (APD) attached to the monochromator. We used a Si-APD instead of a pyroelectric detector in order to detect the much weaker SPDC signal. From the maximum intensities of the wavelength tuning plots, the $(d_{33}/d_{31})_{SPDC}$ ratio was estimated.

III. RESULTS AND DISCUSSION

3.1. SHG Measurements

Figure 2 (left) shows the temperature tuning SHG output for the 5th order QPM type-0 SHG power. The fundamental input pulse energy was 40 μJ at 990.6 nm. The experimental QPM peak was obtained at 58°C which is slightly shifted from the theoretical QPM temperature of 55°C calculated using the Sellmeier equation for the extraordinary wave [15]. However, the experimental temperature bandwidth was ~50°C which is much greater than the theoretical temperature bandwidth of 1.9°C. This large difference could be explained by considering the broad bandwidth of the fundamental input provided by the OPG-OPA system. The

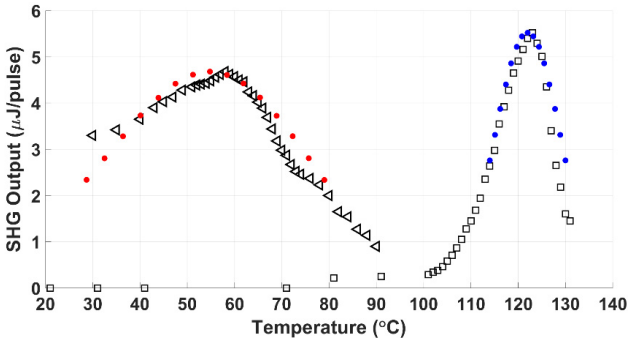

FIG. 2. SHG power versus temperature for type-0 pumped at 990.6 nm (left) and type-1 pumped at 970.8 nm (right). Open triangles: type-0 data, open squares: type-1 data, dots: Type-0 (red), Type-1 (blue) QPM bands calculated based on Sellmeier equations [15] for fifteen different wavelengths within each input fundamental band.

FWHM bandwidth of the pump was 4 nm centered at 990.6 nm. Each of the wavelength components within the fundamental bandwidth would be quasi-phase-matched at a different temperature, contributing to the SHG temperature bandwidth. To verify this, we took fifteen wavelength components within the ±2 nm band from the fundamental center wavelength, calculated their corresponding QPM temperatures, and then compared it with the experimental result. The calculated and experimental results were in agreement with each other as seen in Fig. 2 (left). The 5th order SHG output after filtering out the pump was measured to be 4.68 μJ.

For the 1st order QPM type-1 SHG, the fundamental input energy was 40 μJ (same as in type-0 above) at 970.8 nm. Figure 2 (right) shows the experimental and calculated type-1 SHG temperature tuning curves. The SHG energy was maximal at 122°C, while the theoretical QPM temperature was calculated as 60°C. This large shift could be attributed to a significant difference between the actual refractive index of $MgO:LiNbO_3$ and the one predicted by the Sellmeier equation, and/or to a small deviation of poling period from the designed value during the fabrication process. The ordinary index (n_o) in the Sellmeier equation was up-shifted by 0.01339 to match the experimental results. We chose not to change the extraordinary index (n_e) since the experimental results of the type-0 SHG agreed reasonably with the theory, and n_o has much smaller temperature dependence than n_e for $MgO:LiNbO_3$ [17, 18]. The theoretical bandwidth of the type-1 SHG was 0.21°C, while in experiment it was 12°C. The broader bandwidth could be explained by the broadband nature of our fundamental input as in the type-0 case. The 1st order QPM SHG output energy was measured as 5.52 μJ.

Since the SHG experiments have been performed with the same fundamental pump energies for the same sample, the (d_{33}/d_{31})-ratio can be obtained by taking the ratio of the properly normalized SHG outputs as shown in Table 1.

For a given input fundamental power and PPLN length, the nonlinear coefficient is related to the QPM SHG output power by the following expression,

$$d \propto \frac{m}{\sin(\pi m D)} \sqrt{1.26(\text{SHG output power})} \quad (2)$$

where d is the nonlinear coefficient tensor element d_{33} (type-0) or d_{31} (type-1), m is the QPM order, and D is the duty ratio of the $\chi^{(2)}$-grating [19]. A factor of 1.26 was inserted to consider the effect of bandwidth of the fundamental input which is much broader than the QPM bandwidths. Type-1 SHG has a broader wavelength bandwidth than type-0 SHG as compared in the 'QPM bandwidth' column in Table 1 [15]. For our sample, we measured $D = 0.483$ on average which deviates from the ideal value of $D = 0.5$. This deviation was taken into consideration by the factor $m/\sin(\pi m D)$ in Eq. (2). It is obvious that this scaling factor would be different for type-0 and type-1 interactions in our experiment as their QPM orders are different ($m = 5$ and 1, respectively). The scaling factor turned out to be 5.18 and 1.00 for type-0 and type-1 interaction, respectively. The resulting (d_{33}/d_{31})-ratio was 5.35.

It should be noted that we could minimize the effects of several experimental artifacts such as reflections at the crystal surfaces and the input beam profile in the above comparison since the two experiments were performed at similar wavelengths. We also note that the use of a source with a narrow-linewidth can reduce the uncertainty involved in the above evaluation since the SHG output is directly affected by the fundamental input linewidth when it is greater than the QPM bandwidth.

3.2. SPDC Measurements

The fundamental input wavelengths for the 5th order type-0 SPDC and the 1st order type-1 SPDC were 495.3 nm and 485.4 nm, respectively. We used the same fundamental input energy of 190 μJ/pulse for both cases. Non-degenerate SPDC was obtained in each case so that the obtained signal bands are well within the detectable spectral range of the Si-APD. Figure 3(a) depicts the experimental and theoretical type-0 SPDC spectra. The experimental peaks were obtained at 53°C, while the theoretical temperature was calculated as 69°C to generate the same peak. As in the type-0 SHG temperature-tuning curves, the experimental spectrum was much broader than the theoretical one, which could be justified by taking into account the fundamental input bandwidth. The spectral region between 985 nm and 1020 nm could be attributed to the degeneracy condition that occurs at a pump wavelength of 495.9 nm within the fundamental band. This coincides with the theoretical degeneracy condition that is indicated by the gap between the theoretical signal and idler bands. The idler could not be detected as it was cut off by the spectral response of the Si-APD. We measured a current of 120 nA when the Si-APD detected the 5th order QPM type-0 SPDC signal output in the narrow window of 4 nm, centered at 928 nm set by the monochromator.

The experimental and theoretical spectra of the type-1 SPDC is shown in Fig. 3(b). In this experiment, the SPDC

TABLE 1. Parameters used in the estimation of (d_{33}/d_{31})-ratio from the measured SHG output

	λ_{pump} (nm)	QPM order	SHG output (μJ/p)	QPM bandwidth (nm)	$m/\sin(\pi m D)$ (D = 0.483)	d_{33}/d_{31}
Type-0	990.6	5	4.68	0.0747	5.18	5.35
Type-1	970.8	1	5.52	0.0943	1.00	

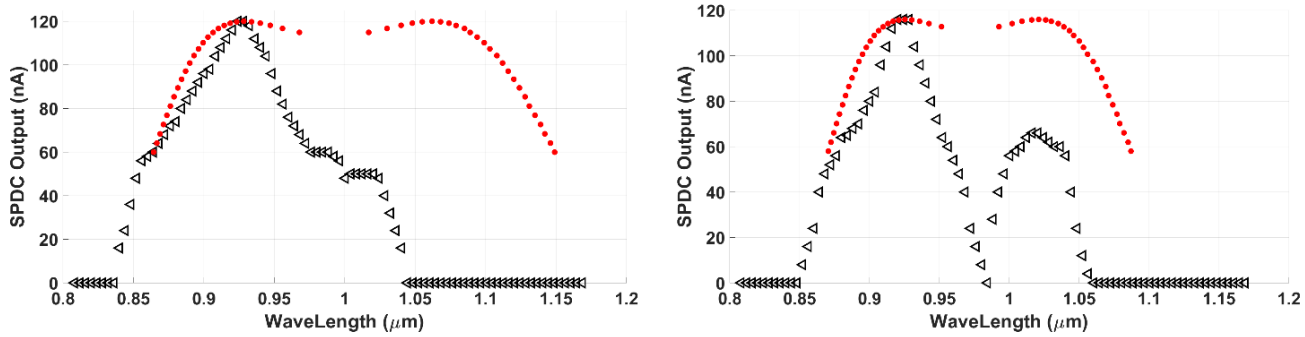

(a) (b)

FIG. 3. Type-0 QPM SPDC spectrum pumped at 495.3 nm, 53°C (a), and type-1 QPM SPDC spectrum pumped at 485.4 nm, 122°C (b). Open triangles: data. Dots: QPM bands calculated based on Sellmeier equations [15] for thirty different wavelengths within the input fundamental bands. The cut-off of Si-APD starts from ~1050 nm.

spectrum was obtained at 122°C, while the theoretical temperature was calculated as 61°C to generate the same peak, which can be explained the same way as in the previously mentioned type-1 SHG experiment. The wider bandwidth experimental spectrum of the signal could be justified in view of the fundamental input linewidth as explained previously. We chose to ignore the strength idler band while calculating the (d_{33}/d_{31})-ratio because of the following reasons. Firstly, since the signals bands generated by the type-0 and type-1 SPDC were similar, the (d_{33}/d_{31})-ratio was obtained by comparing the respective signal strengths and hence we ignored the idler. Secondly, the idler was affected by the cut-off of the Si-APD. We measured a current of 116 nA when the Si-APD detected the 1st order QPM type-1 SPDC signal output in the narrow window of 4 nm, centered at 925 nm set by the monochromator.

The SPDC experiments have been performed with the same fundamental pump energies, the (d_{33}/d_{31}) can be obtained by taking the ratio of the output SPDC signal currents as shown in Table 2.

As in the SHG experiment, the duty ratio was taken into consideration in estimating the (d_{33}/d_{31})-ratio by modifying Eq. (2) as

$$d \propto \frac{m}{\sin(\pi m D)} \sqrt{(\text{SPDC output current})} \tag{3}$$

In SPDC the broad bandwidth of the pump was not included in the correction, because each spectral component in the pump would generate its own QPM signal band in contrast to SHG. The scaling factor $m/\sin(\pi m D)$ has the same value as in SHG.

In the above comparison, the effects of several experimental artifacts such as reflections at the crystal surfaces and the input beam profile are minimized as in the SHG experiments, since we used similar pump wavelengths and detected the signals also at similar wavelengths in the two SPDC experiments.

As a result, SHG and SPDC gave us similar (d_{33}/d_{31})-ratio. The deviation between $(d_{33}/d_{31})_{SHG}$ and $(d_{33}/d_{31})_{SPDC}$ ratios was only 1.5%, which is within the uncertainty range of our power measurement. Our (d_{33}/d_{31}) ratio of 5.35 (from SHG) can be compared with the values obtained by Shoji *et al*. [10], giving a discrepancy of 6%. However, because a ~10% uncertainty is always involved in this kind of experiments relying on the power measurements, it would not be meaningful to discuss a less than 10% error in the evaluation of d-values.

IV. CONCLUSION

In summary, we obtained (d_{33}/d_{31}) ratios in 5% MgO:PPLN crystal by directly measuring the output powers of the quasi-phase-matched SHG and SPDC processes. The results were in good agreement with the previously established values by Shoji *et al*. within the experimental uncertainty. Hence, we conclude that our quasi-phase-matching method offers a simpler, easier and economical approach to estimate the ratio of the nonlinear tensor components when compared to the previously reported procedures. An interesting observation seen in our results was the need to scale n_o value to match theory and experimental results making us believe that the Sellmeier equation of n_o needs to be corrected which would be an interesting subject for further study.

ACKNOWLEDGMENT

This work was supported by a 2-Year Research Grant of Pusan National University.

REFERENCES

1. P. A. Franken, A. E. Hill, C. W. Peters, and G. Weinreich, "Generation of optical harmonics," Phys. Rev. Lett. **7**, 118-120 (1961).
2. J. R. Schewesyg, M. Falk, C. R. Phillips, D. H. Jundt, K. Buse, and M. M. Fejer, "Pyro-electrically induced photo-refractive damage in magnesium-doped lithium niobate crystals," J. Opt. Soc. Am. B. **28**, 1973-1987 (2011).
3. H.-H. Lim, O. Prakash, B.-J. Kim, K. Pandiyan, M. Cha, and B. K. Rhee, "Ultra-broadband optical parametric generation and simultaneous RGB generation in periodically poled lithium niobate," Opt. Express **15**, 18294-18299 (2007).
4. Y. Gan, Y. Lu, Q. Xu, and C. Q. Xu, "Compact integrated green laser module for Watt-level display applications," IEEE Photon. Technol. Lett. **25**, 75-77 (2013).
5. A. Barh, P. T. Lichtenberg, and C. Pederson, "Thermal noise in mid-infrared broadband upconversion detectors," Opt. Express **26**, 3249-3259 (2018).
6. D. A. Bryan, R. Gerson, and H. E. Tomaschke, "Increased optical damage resistance in lithium niobate," Appl. Phys. Lett. **44**, 847-849 (1984).
7. D. Georgiev, V. P. Gapontsev, A. G. Dronov, M. Y. Vyatkin, A. B. Rulkov, S. V. Popov, and J. R. Taylor, "Watt-level frequency doubling of a narrow line linearly polarized Raman

TABLE 2. Parameters used in the estimation of (d_{33}/d_{31})-ratio from the measured SPDC output

	λ_{Pump} (nm)	QPM order	SPDC output (nA)	$m/\sin(\pi m D)$ (D = 0.483)	d_{33}/d_{31}
Type-0	495.3	5	120	5.18	5.27
Type-1	485.4	1	116	1.00	

fiber laser to 589 nm," Opt. Express **13**, 6772-6776 (2005).
8. H. Furuya, A. Morikawa, K. Mizuuchi, and K. Yamamoto, "High- beam-quality continuous wave 3W green-light generation in bulk periodically poled MgO:$LiNbO_3$," Jpn. J. Appl. Phys. **45**, 6704-6707 (2006).
9. R. C. Eckardt, H. Masuda, Y. X. Fan, and R. L. Byer, "Absolute and relative nonlinear optical coefficients of KDP, KD*P, BaB_2O_4, $LiIO_3$, MgO:$LiNbO_3$, and KTP measured by phase-matched second-harmonic generation," IEEE J. Quantum Electron. **26**, 922-933 (1990).
10. I. Shoji, T. Kondo, A. Kitamoto, M. Shirane, and R. Ito, "Absolute scale of second-order nonlinear-optical coefficients," J. Opt. Soc. Am. B **14**, 2268-2294 (1997).
11. R. C. Miller, W. A. Nordland, and P. M. Bridenbaugh, "Dependence of second-harmonic-generation coefficients of $LiNbO_3$ on melt composition," J. Appl. Phys. **42**, 4145-4147 (1971).
12. M. M. Choy and R. L. Byer, "Accurate second-order susceptibility measurements of visible and infrared nonlinear crystals," Phys. Rev. B **14**, 1693-1706 (1976).
13. H. Vanherzeele and J. D. Bierlein, "Magnitude of the nonlinear-optical coefficients of $KTiOPO_4$," Opt. Lett. **17**, 982-984 (1992).
14. E. C. Cheung, K. Koch, G. T. Moore, and J. M. Liu, "Measurements of second-order nonlinear optical coefficients from the spectral brightness of parametric fluorescence," Opt. Lett. **19**, 168-170 (1994).
15. O. Gayer, Z. Sacks, E. Galun, and A. Arie, "Temperature and wavelength dependent refractive index equations for MgO-doped congruent and stoichiometric $LiNbO_3$," Appl. Phys. B, **91**, 343-348 (2008).
16. V. G. Dmitreiv, G. G. Gurzadyan, D. N. Nikogosyan, *Handbook of nonlinear optical crystals* (Springer, 1999).
17. N. Umemura and D. Matsuda, "Thermo-optic dispersion formula for the ordinary wave in 5 mol% MgO doped $LiNbO_3$ and its application to temperature insensitive second-harmonic generation," Opt. Commun. **367**, 167-173 (2016).
18. N. Umemura, D. Matsuda, T. Mizuno, and K. Kato, "Sellmeier and thermo-optic dispersion formulas for the extraordinary ray of 5 mol% MgO-doped congruent $LiNbO_3$ in the visible, infrared, and terahertz regions," Appl. Opt. **53**, 5726-5732 (2014).
19. M. M. Fejer, G. A. Magel, D. H. Jundt, and R. L. Byer, "Quasi-phase-matched second harmonic generation: tuning and tolerances," IEEE J. Quantum Electron. **28**, 2631-2654 (1992).